Mapping dominant-negative mutations of anthrax protective antigen by scanning mutagenesis

Michael Mourez*†, Ming Yan*†, D. Borden Lacy*, Lisa Dillon‡, Lori Bentsen§, Amy Marpoe§, Clémence Maurin*, Eileen Hotze§, Darran Wigelsworth*, Ruth-Anne Pimental*, Jimmy D. Ballard‡, R. John Collier*¶, and Rodney K. Tweten§‖

*Department of Microbiology and Molecular Genetics, Harvard Medical School, 200 Longwood Avenue, Boston, MA 02115; ‡Department of Botany and Microbiology, University of Oklahoma, 770 Van Vleet Oval, Norman, OK 73072; and §Department of Microbiology and Immunology, University of Oklahoma Health Sciences Center, 940 Stanton L. Young Boulevard, Oklahoma City, OK 73104

Contributed by R. John Collier, September 30, 2003

The protective antigen (PA) moiety of anthrax toxin transports edema factor and lethal factor to the cytosol of mammalian cells by a mechanism that depends on its ability to oligomerize and form pores in the endosomal membrane. Previously, some mutated forms of PA, designated dominant negative (DN), were found to coassemble with wild-type PA and generate defective heptameric pore-precursors (prepores). Prepores containing DN–PA are impaired in pore formation and in translocating edema factor and lethal factor across the endosomal membrane. To create a more comprehensive map of sites within PA where a single amino acid replacement can give a DN phenotype, we used automated systems to generate a Cys-replacement mutation for each of the 568 residues of PA_{63}, the active 63-kDa proteolytic fragment of PA. Thirty-three mutations that reduced PA's ability to mediate toxicity at least 100-fold were identified in all four domains of PA_{63}. A majority (22) were in domain 2, the pore-forming domain. Seven of the domain-2 mutations, located in or adjacent to the $2\beta_6$ strand, the $2\beta_7$ strand, and the $2\beta_{10}$-$2\beta_{11}$ loop, gave the DN phenotype. This study demonstrates the feasibility of high-throughput scanning mutagenesis of a moderate sized protein. The results show that DN mutations cluster in a single domain and implicate $2\beta_6$ and $2\beta_7$ strands and the $2\beta_{10}$–$2\beta_{11}$ loop in the conformational rearrangement of the prepore to the pore. They also add to the repertoire of mutations available for structure–function studies and for designing new antitoxic agents for treatment of anthrax.

The ability of *Bacillus anthracis* to cause disease depends on two major virulence factors: a secreted tripartite toxin, which is believed to cause the main symptoms of anthrax, and a poly(D-glutamic acid) capsule, which inhibits phagocytosis of the bacterium (1). Recent advances in understanding the structure and mode of action of the toxin have provided novel approaches to treating anthrax (2).

Anthrax toxin is a member of the *binary* bacterial toxins, a subset of intracellularly acting toxins in which the enzymatic and receptor-binding moieties are secreted by the bacteria as discrete monomeric proteins (3, 4). These proteins assemble at the surface of receptor-bearing eukaryotic cells to form toxic hetero-oligomeric complexes. The complexes are internalized and delivered to an acidic compartment, where the receptor-binding moiety inserts into the membrane and mediates translocation of the enzymatic moiety to the cytosol. Within the cytosol, the enzymatic moiety modifies a molecular target, disrupting cell physiology and causing cytopathic effects. Anthrax toxin consists of two enzymatic moieties, edema factor (EF; 89 kDa) and lethal factor (LF; 90 kDa), and a single receptor-binding moiety, protective antigen (PA; 83 kDa), named for its ability to elicit protective immunity. EF is a Ca^{2+} and calmodulin-dependent adenylate cyclase (5, 6), and LF is a Zn^{2+}-dependent protease that cleaves mitogen-activated protein kinase kinases (7, 8).

After binding to its cellular receptor (9), PA is cleaved by the furin class of cellular proteases (10). This removes a 20-kDa fragment, PA_{20}, from the N terminus and leaves the complementary C-terminal fragment, PA_{63} (63 kDa), bound to the receptor. PA_{63} then spontaneously oligomerizes to form a ring-shaped heptamer (11). EF and LF bind competitively to identical sites on oligomeric PA_{63} (12, 13), yielding a series of toxic complexes containing one to three molecules of EF and/or LF bound per PA_{63} heptamer (14). Oligomerization of PA_{63} triggers endocytosis (15, 16) and trafficking to an endosomal compartment (17, 18). After acidification of the endosomal compartment, the PA_{63} heptamer undergoes a conformational change that allows it to insert into the membrane, form a cation-selective pore, and translocate EF/LF to the cytosol (19–21).

The crystallographic structure of intact PA has been solved and shows that the protein is organized into four domains (Fig. 1) (22). Domain 1, the N-terminal domain, contains the furin cleavage site and therefore encompasses PA_{20}. That portion of domain 1 within PA_{63}, termed domain 1′, contains two calcium atoms and participates in EF/LF binding (13) and oligomerization (23). Domain 2 contains a flexible loop ($2\beta_2$–$2\beta_3$) that is believed to form the transmembrane region of the pore. Ion conductance experiments on Cys-substitution mutants strongly suggest that the $2\beta_2$–$2\beta_3$ loops from the seven subunits of the prepore combine to form a transmembrane 14-strand β-barrel (24, 25). Domain 3 is involved in oligomerization (23), and domain 4, the C-terminal domain, contains the receptor-binding site (9, 26, 27). In addition to monomeric PA, the structure of a soluble form of the PA_{63} heptamer has been solved (22); it is believed to represent the conformation of the heptamer before pore formation and has been termed the prepore.

PA mutants blocked at discrete steps of the intoxication process have given important insights into structure–function relationships of PA, and some of these mutants have properties that may make them useful in treating anthrax. Of particular interest are mutations that make the protein dominantly negative (DN), thereby converting it into a potent antitoxin (28). DN–PA cooligomerizes with wild-type PA_{63} and inhibits its ability to form pores and mediate translocation. Point mutations at D425 and F427, a deletion or substitution of the $2\beta_2$–$2\beta_3$ loop, or combinations of these mutations, have been shown to confer varying degrees of DN activity on PA (28–30).

The analysis of large arrays of PA mutants has recently become feasible, following identification of ways to obtain small-scale preparations of PA mutants and screen them rapidly and reliably for defects in PA functions (23). Primarily to search PA for additional DN sites, we developed a protocol to mutate each of the 568 amino acids of PA_{63} to Cys and characterize the resulting mutants. We restricted our study to PA_{63} because PA_{20} does not appear to play a role in intoxication besides preventing

BIOCHEMISTRY

Abbreviations: PA, protective antigen; EF, edema factor; LF, lethal factor; DN, dominant negative; DTA, diphtheria toxin A-chain; LF_N, N-terminal domain of LF; CHO, Chinese hamster ovary.

†M.M. and M.Y. contributed equally to this work.

¶R.J.C. holds equity in PharmAthene, Inc. (Annapolis, MD).

‖To whom correspondence should be addressed. E-mail: rod-tweten@ouhsc.edu.

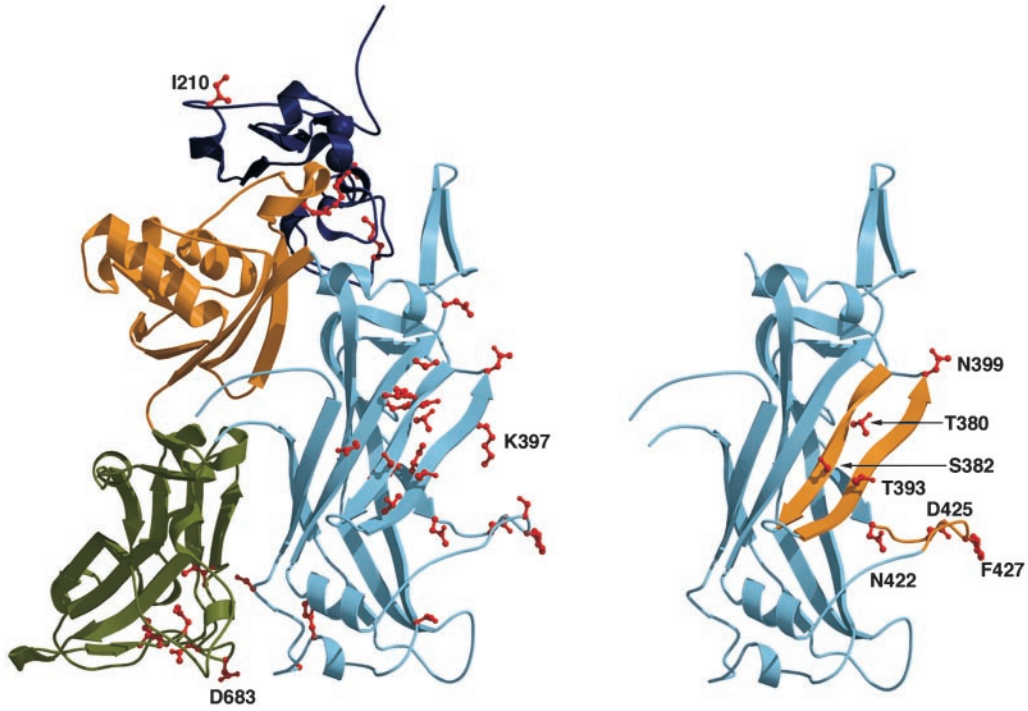

Fig. 1. Mapping the 33 defective mutations on the structure of PA_{63}. (*Left*) A monomeric subunit of the PA_{63} prepore heptamer is shown with domain 1′ and the calcium ions in dark blue, domain 2 in light blue, domain 3 in yellow, and domain 4 in green. The 33 residues for which a mutated PA was defective yet expressed are colored red. (*Right*) The mutants with a DN effect are mapped onto domain 2 and indicated in red. The mutants map to three key structural elements indicated in yellow: the $2\beta_6$ strand (T380 and S382), the $2\beta_7$ strand (T393 and N399), and the $2\beta_{10}$–$2\beta_{11}$ loop (N422). D425 and F427, also shown in the $2\beta_{10}$–$2\beta_{11}$ loop, were identified as sites of DN mutants (28).

toxin assembly in solution. Cys-replacements were chosen because this amino acid is absent from PA and because the thiol-containing side chain is amenable to specific derivatization, facilitating structure-function studies (24, 25, 31–33).

We first screened for mutations that a caused large (>100-fold) reduction in PA's ability to mediate toxicity. Such mutations were identified in all four domains, but a majority were in domain 2. Mutations conferring the DN phenotype were found exclusively within domain 2, in the $2\beta_6$ strand, the $2\beta_7$ strand, or the $2\beta_{10}$–$2\beta_{11}$ loop. Because DN mutants prevent the conformational transition of PA_{63} from the prepore to the pore state, we conclude that these structural elements play major roles in this change. Some of the newly identified mutations may be useful in designing new antitoxins for treatment of anthrax.

Materials and Methods

Mutagenesis of PA. The mutagenic oligonucleotides were each designed to have a melting temperature of ≈85°C, 33 nt long, with the mutagenic site located centrally, and the 3′ end being GC rich if possible. The oligonucleotides were synthesized with a MerMade automated system (Plano, TX) in a 96-well plates and checked by using capillary electrophoresis. The mutagenesis of PA-pET22b was performed by using a GenAmp 9700 PCR system (Applied Biosystems, Foster City, CA) according to the protocol provided by the Site Directed Mutagenesis QuikChange kit (Stratagene). The success rate after the first round of PCR was ≈90% when this AT rich template was used. An aliquot of mutagenized product was used to transform *Escherichia coli* XL-1 Blue Supercompetent cells (Stratagene), and the bacteria were spread on LB agar plates containing 100 μg/ml ampicillin.

After overnight incubation, two colonies were picked from each mutagenesis reaction into 96-deep-well plates containing 1.5 ml of selective broth. Hence, 192 clones were picked and sequenced for each set of 96 mutants. After overnight growth in 96-deep-well plates (2 ml culture volume), plasmid DNA purification was performed by using an automated liquid handling machine, the Biomeck 2000 workstation (Beckman, Fullerton, CA) to perform a modified alkaline lysis and extraction of the plasmid DNA (www.microgen.ouhsc.edu/manuals_protocols/if_isol_dna_temp_b.htm). The isolated plasmid DNA was used to sequence the region containing the mutation and to provide a permanent stock of the plasmid DNA if the mutation was confirmed by DNA sequence analysis. The presence of the mutation was confirmed by DNA sequence analysis using an Applied Biosystems 3700 capillary DNA sequencer. Typically the success rate of both clones containing the mutation was 99%. DNA bearing the desired mutation was used to transform *E. coli* Tuner (DE3) (Novagen, Madison, WI), made chemically competent (Zymo Research, Orange, CA), and the resulting clones were kept for further study. The full sequence of PA was not checked for each mutant, and it is therefore possible that some mutants may have additional unwanted mutations. However, the full sequences of the 33 defective mutants described herein were confirmed.

During the process of mutagenesis, some minor problems arose that primarily centered on the production of the mutated template by the QuikChange mutagenesis methods. The problems were primarily concerned with the PCR and the lack of production of the mutated template. Typically, these problems were solved by altering the template and/or the primer concentration or the PCR cycle parameters, although the exact conditions typically varied for each case. In cases in which these approaches were ineffective, the mutagenic oligonucleotides were redesigned by lengthening the primer by adding additional bases, preferably including G or C if possible, to the 3′ end to ensure its hybridization with the proper site on the template and to anchor the 3′ end of the primers. All DNA sequencing and

oligonucleotide synthesis was performed by the Laboratory for Genomics and Bioinformatics in the Department of Microbiology and Immunology at the University of Oklahoma Health Sciences Center (http://microgen.ouhsc.edu).

Screening for Inactive Mutants. Bacterial cultures grown in a 96-deep-well plate containing 1 ml of selective broth were induced for protein expression with 0.1 mM isopropyl β-D-thiogalactoside overnight at 16°C. Strains containing plasmids allowing the expression of wild-type PA or an empty plasmid were used as positive and negative controls, respectively. Whole cell lysates were prepared by adding T7 phage at a multiplicity of infection of 3 to each culture and shifting them to 37°C, according to a previously described method (23). Bacterial debris was pelleted by centrifugation, and 10 μl of the supernatants containing the PA mutants was mixed with 90 μl of cell culture medium (RP-10 medium with 10% FCS) containing 1.5 μg of purified recombinant LF. The mixtures were added to 96-well plates containing 5×10^5 RAW 264.2 macrophage cells per well, and the plates were incubated for 4 h. Macrophage viability was assayed with the CCK-8 vital stain (Dojindo Laboratories, Gaithersburg, MD).

Strains expressing inactive mutants were tested further. Bacteria were grown in 5 ml of selective broth in individual tubes, and protein expression was induced with 0.2 mM isopropyl β-D-thiogalactoside for 3 h at 30°C. Periplasmic fractions were prepared according to the osmotic shock procedure (33) and recovered in 500 μl of 5 mM $MgSO_4$/5 mM DTT containing a mixture of protease inhibitors (Complete EDTA-free, Roche Applied Sciences). The periplasmic extracts were serially diluted in cell culture medium (HAM-F12 medium containing 10% calf serum), and 25 μl of each dilution was mixed with 100 μl of medium containing 10^{-9} M purified LF_NDTA (LF_N, N-terminal domain of LF; DTA, diphtheria toxin A-chain). The mixtures were added to 96-well plates containing 2.5×10^5 Chinese hamster ovary (CHO)-K1 cells per well, and the plates were incubated overnight. Cell viability was assayed with the WST1 vital stain (Roche Applied Sciences).

The relative amount of each inactive mutant PA in periplasmic extracts was determined by Western blotting using polyclonal antibodies directed against PA and compared with the amount of PA found in an extract containing wild-type PA by densitometry analysis.

DN Inhibition and Animal Protection Assays. The assay for DN inhibitor activity was performed as before (28, 30) with a fixed amount of PA (2×10^{-10} M) and LF_NDTA (10^{-9} M) and increasing amounts of each PA mutant purified as described (30) or periplasmic fractions containing PA mutants.

The animal protection was performed as described (28). Fisher 344 male rats (Harlan Laboratories, Haslett, MI), 250–300 g, were challenged intravenously with 40 μg of purified PA and 8 μg of purified LF in the presence (three rats) or absence (three rats) of 40 μg of purified T393C. The rats were monitored up to a week after the injection and were killed if moribund.

Characterizations of PA Mutants. Heptamer formation, LF_N binding and translocation, $^{86}Rb^+$ release, and cell binding assays are briefly described below but were fully detailed elsewhere (9, 30). Assays were performed with periplasmic fractions containing PA mutants or pure proteins obtained as described (30). Purified proteins, 2 μg, were nicked by adding a limited amount of trypsin and used for the assays. Because nicking of PA is not possible with unpurified preparations, this step was replaced when using periplasmic extracts by incubating CHO-K1 cells with extracts containing ≈2 μg of PA, as judged by Western blot, at 37°C for 45 min. This allowed cellular proteolytic activation of PA.

Heptamer formation was assayed with nicked, purified PA by incubating the protein with an equimolar amount of LF_N and separating the mixture by native PAGE. When assaying SDS-resistance of the heptamer, the pH of the mixture was lowered to pH 5.0 and the samples separated by SDS/PAGE. LF_N binding and translocation was assayed by incubating nicked proteins or periplasmic fractions with CHO-K1 cells for 1 h. The cells were washed with PBS, and radiolabeled LF_N was added for 1 h. The cells were again washed and then pulsed for 1 min with a buffer at pH 5 and either treated with pronase or buffer alone. The cells were then lysed and the amount of radioactivity counted. Release of $^{86}Rb^+$ was assayed by adding nicked purified protein or periplasmic fractions to CHO-K1 cells loaded with $^{86}Rb^+$. The cells were then incubated with a pH 5 buffer for 30 min on ice and the amount of released radioisotope counted. Cell binding of PA was evaluated by adding periplasmic extracts containing PA mutants to CHO-K1 cells. The amount of bound PA was revealed by Western blot. For each assay, positive and negative controls were performed corresponding to purified wild-type PA and buffered medium alone, respectively.

Results

Mutagenesis. To generate a complete library of Cys mutants of PA_{63} we used the QuikChange (Stratagene) method to generate point mutations, but performed it in conjunction with automated systems currently used for high-throughput DNA sequencing. The *pag* gene encoding PA is AT rich (34% GC) and did not present significant technical hurdles. Automated systems were used to synthesize the mutagenic oligonucleotide pairs, and the quality of mutagenic oligonucleotides were confirmed by automated capillary electrophoresis. In this manner, a full plate could be processed in a day, and the oligonucleotides needed for complete mutagenesis of PA_{63} could be synthesized and checked in 12 days. After manually performing the PCR mutagenesis in 96-well plates and transforming the resulting mutated plasmids into *E. coli*, automation was again used for preparing DNA from the colonies and sequencing of the region of interest. Clones bearing the desired mutation were used for functional screens. We used this protocol to generate 568 mutants, corresponding to the replacement of every amino acid of PA_{63} with Cys.

Toxicity and Expression Levels of the Mutants. Because of the large number of mutants to be tested, functional defects were identified in a two-step process (Table 3, which is published as supporting information on the PNAS web site). In the first stage, bacteria expressing the mutants were grown in 96-deep-well plates, and whole-cell lysates were prepared by adding T7 phage (23). The lysates were mixed with cell culture medium containing purified LF and incubated with RAW murine macrophages (34). After 4 h, the viability of the macrophages was assayed with a vital stain.

Mutants of PA that lacked the capacity to facilitate LF-mediated killing of macrophage were subjected to the second screening step. Bacteria were grown in individual tubes, and periplasmic fractions were obtained by osmotic shock. Serial dilutions of the periplasmic preparations were mixed with cell culture medium containing purified LF_NDTA and incubated with CHO cells. LF_NDTA contains the catalytic chain of DTA fused to the LF_N (35). This fusion protein follows the same PA-dependent route as LF or EF to the cytosol, where the DTA moiety catalyzes the ADP-ribosylation of elongation factor-2, blocking protein synthesis and causing cell death. After an overnight incubation with the samples, cells were assayed for viability with a vital stain.

When we used extracts containing wild-type PA prepared under the same conditions as a standard, we found that the first assay detected up to ≈100-fold reduction of toxicity, and the second accurately scored even greater reductions, of 200- to 10,000-fold. For all of the mutants found to be defective in the

Table 1. Amino acid residues at which Cys substitutions inhibited PA activity by at least 100-fold

Domain	Residues
1	I210, K225, T240, K245
2	S337, G342, W346, T357, I364, P379, T380, S382, T390, T393, K397, N399, Y411, I419, A420, N422, F427, S248, D451, D453, V455, N458
3	E515
4	I656, N657, I665, N682, D683, L687

The toxicity of the PA mutants was tested by two successive assays as described in the text.

second assay, we evaluated the amounts of PA present in the periplasmic extracts by Western blot analysis, using polyclonal antibody against PA. Those mutants showing <10% of the full-length wild-type PA level were considered to be impaired in expression and were not tested further.

The two-step approach had several advantages. The use of two independent methods to evaluate the toxicity of the mutants strengthened the conclusion that a mutant was defective. The second method was more time consuming and labor intensive than the first, but detected lower levels of residual activity. Thus, the two-step approach avoided performing the more time consuming method for every mutant and yet enabled us to differentiate the strongly defective mutants (those showing >100-fold reduction of toxicity) from those that were mildly defective. The latter were difficult to identify by screening, because they could not be easily discriminated from mutants that were functional but were expressed at marginally reduced levels. One should note that several mutants with mild defects have been instrumental in earlier structure–function studies (13, 23), and such mutants were ignored in our approach.

Of the 134 mutants scored as defective by this two-step protocol, 101 were impaired in expression (Table 3). We did not experimentally address the basis of defective expression, but this defect was seen primarily in residues that were buried and/or involved in contacts with other amino acids, leading us to believe that loss of stability was responsible in most cases. Domain 1 showed a larger percentage of residues where mutation caused defective expression (32%, compared with 21%, 11%, and 9%, respectively, for the remaining domains). Most of the residues are involved in binding the two Ca^{2+} atoms, consistent with the notion that these atoms function primarily in stabilizing this domain. Curiously, the D425C mutation in domain 2 significantly impaired expression, although other substitutions at this site appear to be tolerated.

Thirty three mutants (6% of the total number of mutants tested) were both strongly defective and well expressed. As shown in Table 1 and Fig. 1*A*, the 33 mutations were distributed among the four domains of PA. Strikingly a majority, 22, were in domain 2.

Some Inactive Mutants Are Dominant. We tested serial dilutions of periplasmic preparations containing the 33 inactive mutants for ability to inhibit the toxicity of a mixture of PA and LF_NDTA toward CHO cells at ratios of mutated to wild-type PA up to 8:1. Those that showed measurable inhibitory activity under these conditions were defined, for the purpose of this study, as DN [We prefer for the time being to use this operational definition of "dominant negative." There is no absolute scale of toxicity; values are always dependent on the conditions of assay and the standard employed.] Nine preparations of mutant PA were inhibitory: I364, T380, S382, T393, K397, N399, Y411, N422, and F427. These mutations were all located within domain 2. Seven of these mutants were purified for further characterization; because mutations of K397 and F427 had been documented earlier, they were omitted.

Like the DN mutants characterized earlier, the purified DN Cys-mutants showed defects specifically in pore formation and translocation (Table 2). The trypsin-activated proteins heptamerized normally in solution in the presence of LF_N, as shown by native PAGE, and receptor-bound mutant PAs on the CHO-K1 cell surface were unimpaired in binding radiolabeled LF_N. Under acidic conditions, PA_{63} heptamers in solution failed

Table 2. Characterization of the DN mutants

Mutant	LF_N binding	LF_N translocation	Pore formation	Heptamer formation	SDS-resistant heptamer
WT	+++	+++	+++	+++	+++
I364C	+++	−	−	+++	−
T380C	+++	−	−	+++	−
S382C	+++	−	−	+++	−
T393C	+++	−	−	+++	−
N399C	+++	−	−	+++	−
Y411C	+++	−	−	+++	+
N422C	+++	−	−	+++	−
D425K*	+++	−	−	+++	−
K397D*	+++	−	−	+++	−
F427A*	+++	−	−	+++	+++

All of the mutants tested showed <0.01 wild-type PA activity in mediating the toxicity of LF_NDTA. LF_N binding is measured as the amount of LF_N bound to CHO cells preincubated with trypsin-nicked PA (nPA). LF_N translocation is the percentage of bound LF_N protected from proteolysis after a pulse at pH 5. Pore formation is measured as the amount of $^{86}Rb^+$ released from preloaded cells incubated with nPA and pulsed at pH 5. Heptamer formation is visualized by native PAGE of equimolar mixes of nPA with LF_N. Formation of SDS-resistant heptamers is triggered by dropping the pH of the mixes to pH 5 and is visualized by SDS/PAGE. The activities are reported as +++, 75–100%; ++, 25–74%; +, 5–24%, and −, <5% of wild-type levels.
*The data for these mutants are derived from previous experiments (41).

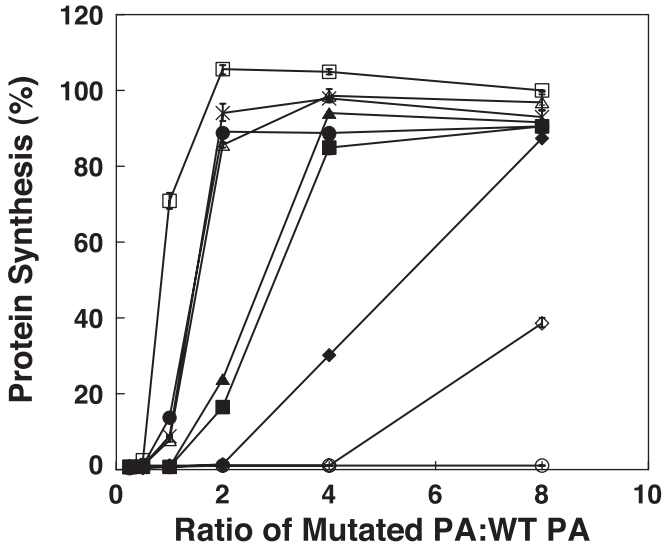

Fig. 2. DN effect of some PA mutants. CHO-K1 cells were incubated with 2×10^{-10} M PA and 10^{-9} M LF_NDTA in the presence of PA mutants or more wild-type PA at various mutant/wild-type PA ratios. The intoxication proceeded for 4 h, at which time protein synthesis was evaluated as described (30). The PA molecules tested are D425K/K397D (□), wild type (○), I364C (◇), S382C (△), N399C (■), T393C (●), T380C (×), N422C(▲), and Y411C (♦).

to convert to the SDS-resistant state characteristic of the pore, and cell-bound mutants did not permeabilize the plasma membrane under such conditions, as determined by $^{86}Rb^+$-release. Finally, PA_{63}-bound radiolabeled LF_N on cells was not translocated to a protease-protected site under acidic conditions.

As shown in Fig. 2, PA bearing T393C, T380C, or S382C showed strong DN activity, only slightly weaker than that of the K397D + D425K double mutant characterized earlier. N399C and N422C showed moderate DN activity, and I364C and Y411C showed weak inhibitory activity.

One of the strongest of the five DN mutants, T393C, was tested for ability to protect Fisher 344 rats from a lethal challenge with a mixture of PA and LF. Like the other DN mutants tested (28), T393C prevented symptoms of intoxication until the time of death, whereas rats challenged with native toxin alone became moribund 75 min after challenge (data not shown).

Discussion

To undertake this project, we developed protocols for high-throughput mutagenesis of a relatively large protein. Complete scanning mutagenesis with Cys, Ala, or random substitutions had been performed before on proteins like LacY (36), HIV-1 protease (37), and other polypeptides (38–40), but the studies on full-length proteins involved multiple rounds of mutagenesis and characterization was conducted over several years. By comparison, our approach involved the complete mutagenesis and initial characterization of 568 PA mutants in <1 year. In this era of genomic-scale studies, the instruments for automation we used are found in many laboratories, and thus our approach could be readily adapted to other proteins.

By using two activity assays sequentially, we were able to screen the resulting mutants rapidly for defects in toxicity. The expression level for each defective mutant was used as a presumptive gauge of its structural stability. In the end, we were able to identify 33 well expressed mutants with defects in toxicity. Mapping these residues to the three-dimensional structure of PA_{63} (Fig. 1*A*) shows that these residues are concentrated on the luminal surface of domain 2. The fact that we kept only strongly defective mutants for analysis undoubtedly caused us to overlook some functionally important residues. Another limitation, not unique to our protocol, resulted from the choice of a single substituting residue, Cys in our case. In contrast to the Cys substitutions, Ala substitutions at selected sites gave different results: Y411A showed strong DN activity; T380A and N399A showed weak DN activity; and N422 and S382A showed no DN activity. At position 393, Cys or Lys gave strong DN activity; Asp or Ala gave moderate DN activity; and Ser gave no DN activity (M.Y. and R.J.C., unpublished data). No mutational profile of inactivation can be considered absolute, however, because any will be specific to some degree to the chosen substituting residue.

Despite these limitations, the fact that many of the 33 residues map to regions previously implicated in functions of EF/LF binding, receptor binding, and/or oligomerization lends support to both the method and the working multistep intoxication model. For instance, the identification of I210C as a functionally defective mutant is consistent with results for a I210A mutant that was previously shown to be impaired in LF_N binding (13). We observed that in periplasmic fractions I210C was unable to bind LF_N on cells but could form pores (data not shown), suggesting that this mutant can bind to cells and oligomerize, and that the resulting heptamers can insert in the membrane but have a defect in LF_N binding. This result confirms that I210 belongs to the LF_N-binding site. Another example is N682C. We previously showed that N682S was unable to bind the cellular receptor of anthrax toxin (9). Likewise, we observed that periplasmic fractions of N682C were affected in binding to cells, and therefore unable to bind LF_N and form pores on cells (data not shown). This confirms that N682 belongs to the receptor-binding site. Lastly, E515C is within the same loop as D512, a residue for which we previously showed a defect in oligomerization upon mutation to Ala or Lys (23). We observed that E515C could bind to cells but did not bind LF_N nor form pores (data not shown), consistent with the hypothesis that this mutant is unable to form heptamers because its oligomerization interface is altered.

The classification of functional defects for some of the other mutations, particularly those affecting residues in domain 2 circumscribing the lumen of the prepore, was not as obvious. We tested the pure proteins or periplasmic fractions containing inactive mutants involving those residues (I364, P379, T380, S382, T390, T393, K397, N399, Y411, I419, A420, N422, F427, S428, D451, D453, V455, and N458) for their ability to bind cells, oligomerize, bind LF_N, and form pores on cells (Table 2 and data not shown). None of these mutants was able to form pores, but all bound LF_N as well as wild type. This observation suggests that they can bind cells and oligomerize to form a prepore but cannot be converted to a pore.

Seven of these mutants, I364C, T380C, S382C, T393C, K397C, N399C, and N422C, were found to act in a DN fashion. At the time this study began, the known DN mutations of PA fell into two categories: (*i*) individual amino acid replacements for either of two residues, D425 and F427; and (*ii*) a multiresidue deletion or substitution of the pore forming, $2\beta_2$–$2\beta_3$ loop. All DN mutations were in domain 2 and specifically affected the related functions of pore formation and translocation. The DN mutants identified in the current study are located in the $2\beta_6$ strand (T380 and S382), the $2\beta_7$ strand (T393 and N399), and the $2\beta_{10}$–$2\beta_{11}$ loop (N422), the last of these also containing D425 and F427 (Fig. 1*B*). The side chains of all of these DN residues are solvent accessible in the prepore, but the strong effects of mutating even a single one of them suggests that they make contacts with other residues in the pore state, or possibly in an intermediate state in the prepore-to-pore transition. Alternatively, a DN mutation might impede the transition by increasing the stability of the prepore, and thus increasing the activation energy. Exploring these mutations further may facilitate the understanding of the prepore-to-pore transition and the translocation process.

The finding that DN mutations are localized exclusively to domain 2 and specifically affect pore formation/translocation is consistent with the current model of anthrax toxin assembly and action. The prepore is believed to convert to the pore in a concerted, presumably cooperative, structural rearrangement of the identical subunits. Thus, the presence of a DN subunit that is unable to undergo the requisite conformational change can apparently block the entire rearrangement.

The individual DN mutations vary in potency and may not be qualitatively different from other domain 2 mutations that affect pore formation/translocation. Rather, they may simply cause greater disruption of the prepore-to-pore transition. Combining various DN mutations with others in domain 2 that either are or are not DN has been shown to enhance DN activity. A noteworthy example is the K397D+D425K double mutant. Whereas K397D by itself does not show DN activity, the K397D+D425K double mutant is among the strongest we have seen and may block translocation at the level of a single mutant subunit per heptamer. The additional domain 2 mutations reported here therefore provide the basis for many other combinations with high DN potency.

The high-throughput approach is amenable to the study of most proteins and can be used to rapidly generate a general view of the functionally important domains of a protein, providing that a functional protein can be expressed and an adequate screening procedure can be used to identify changes in its activity. The choice of amino acid substitution largely depends the objectives of the study. In the present case, cysteine was chosen for two reasons, the first is that no naturally occurring cysteines are present in PA and second, cysteine offers the possibility of attaching sulfhydryl-specific probes at any site of the PA structure for subsequent analyses. Different side chains (e.g., alanine versus cysteine) can result in different phenotypes, as was apparent in these studies. However, if the purpose of a study is to map out functional domains of a protein, then it is unlikely that the choice of amino acid substitution would exclude the identification of a functional domain. In the present study, the substitution of cysteine resulted in the identification of residues in all known functional domains of PA.

In conclusion, we have devised a protocol for high-throughput scanning mutagenesis and demonstrated its efficacy on a moderately large protein of medical importance. Besides yielding a global view of highly vulnerable sites in PA, the current work has provided a set of mutations that will facilitate fine dissection of structure–function relationships of the protein. Such mutations may also be useful for constructing new therapeutics and vaccines against anthrax.

We thank Sen Zhang for the gift of purified PA mutants. This work was supported by Award MIPT106-113-2000-080 from the Oklahoma City National Memorial Institute for the Prevention of Terrorism (MIPT) and the Office of Domestic Preparedness, Department of Homeland Security (to R.K.T.), and by National Institutes of Health Grant AI-22021 (to R.J.C.).

1. Mock, M. & Fouet, A. (2001) *Annu. Rev. Microbiol.* **55,** 647–671.
2. Mourez, M., Lacy, D. B., Cunningham, K., Legmann, R., Sellman, B. R., Mogridge J. & Collier, R. J. (2002) *Trends Microbiol.* **10,** 287–293.
3. Lacy, D. B. & Collier, R. J. (2002) *Curr. Top. Microbiol. Immunol.* **271,** 61–85.
4. Brossier, F. & Mock, M. (2001) *Toxicon* **39,** 1747–1755.
5. Leppla, S. H. (1982) *Proc. Natl. Acad. Sci. USA* **79,** 3162–3166.
6. Drum, C. L., Yan, S. Z., Bard, J., Shen, Y. Q., Lu, D., Soelaiman, S., Grabarek, Z., Bohm, A. & Tang, W. J. (2002) *Nature* **415,** 396–402.
7. Duesbery, N. S., Webb, C. P., Leppla, S. H., Gordon, V. M., Klimpel, K. R., Copeland, T. D., Ahn, N. G., Oskarsson, M. K., Fukasawa, K., Paull, K. D., *et al.* (1998) *Science* **280,** 734–737.
8. Pannifer, A. D., Wong, T. Y., Schwarzenbacher, R., Renatus, M., Petosa, C., Bienkowska, J., Lacy, D. B., Collier, R. J., Park, S., Leppla, S. H., *et al.* (2001) *Nature* **414,** 229–233.
9. Bradley, K. A., Mogridge, J., Mourez, M., Collier, R. J. & Young, J. A. (2001) *Nature* **414,** 225–229.
10. Molloy, S. S., Bresnahan, P. A., Leppla, S. H., Klimpel, K. R. & Thomas, G. (1992) *J. Biol. Chem.* **267,** 16396–16402.
11. Milne, J. C., Furlong, D., Hanna, P. C., Wall, J. S. & Collier, R. J. (1994) *J. Biol. Chem.* **269,** 20607–20612.
12. Mogridge, J., Cunningham, K., Lacy, D. B., Mourez, M. & Collier, R. J. (2002) *Proc. Natl. Acad. Sci. USA* **99,** 7045–7048.
13. Cunningham, K., Lacy, D. B., Mogridge, J. & Collier, R. J. (2002) *Proc. Natl. Acad. Sci. USA* **99,** 7049–7053.
14. Mogridge, J., Cunningham, K. & Collier, R. J. (2002) *Biochemistry* **41,** 1079–1082.
15. Beauregard, K. E., Collier, R. J. & Swanson, J. A. (2000) *Cell. Microbiol.* **2,** 251–258.
16. Liu, S. & Leppla, S. H. (2003) *J. Biol. Chem.* **278,** 5227–5234.
17. Abrami, L., Liu, S., Cosson, P., Leppla, S. H. & Van der Goot, F. G. (2003) *J. Cell. Biol.* **160,** 321–328.
18. Friedlander, A. M. (1986) *J. Biol. Chem.* **261,** 7123–7126.
19. Blaustein, R. O., Koehler, T. M., Collier, R. J. & Finkelstein, A. (1989) *Proc. Natl. Acad. Sci. USA* **86,** 2209–2213.
20. Milne, J. C. & Collier, R. J. (1993) *Mol. Microbiol.* **10,** 647–653.
21. Wesche, J., Elliott, J. L., Falnes, P. O., Olsnes, S. & Collier, R. J. (1998) *Biochemistry* **37,** 15737–15746.
22. Petosa, C., Collier, R. J., Klimpel, K. R., Leppla, S. H. & Liddington, R. C. (1997) *Nature* **385,** 833–838.
23. Mogridge, J., Mourez, M. & Collier, R. J. (2001) *J. Bacteriol.* **183,** 2111–2116.
24. Benson, E. L., Huynh, P. D., Finkelstein, A. & Collier, R. J. (1998) *Biochemistry* **37,** 3941–3948.
25. Nassi, S., Collier, R. J. & Finkelstein, A. (2002) *Biochemistry* **41,** 1445–1450.
26. Brossier, F., Sirard, J. C., Guidi-Rontani, C., Duflot, E. & Mock, M. (1999) *Infect. Immun.* **67,** 964–967.
27. Varughese, M., Teixeira, A. V., Liu, S. & Leppla, S. H. (1999) *Infect. Immun.* **67,** 1860–1865.
28. Sellman, B. R., Mourez, M. & Collier, R. J. (2001) *Science* **292,** 695–697.
29. Singh, Y., Khanna, H., Chopra, A. P. & Mehra, V. A. (2001) *J. Biol. Chem.* **276,** 22090–22094.
30. Yan, M. & Collier, R. J. (2003) *Mol. Med.* **9,** 46–51.
31. Hotze, E. M., Wilson-Kubalek, E. M., Rossjohn, J., Parker, M. W., Johnson, A. E. & Tweten, R. K. (2001) *J. Biol. Chem.* **276,** 8261–8268.
32. Ramachandran, R., Heuck, A. P., Tweten, R. K. & Johnson, A. E. (2002) *Nat. Struct. Biol.* **9,** 823–827.
33. Miller, C. J., Elliott, J. L. & Collier, R. J. (1999) *Biochemistry* **38,** 10432–10441.
34. Hanna, P. C., Acosta, D. & Collier, R. J. (1993) *Proc. Natl. Acad. Sci. USA* **90,** 10198–10201.
35. Milne, J. C., Blanke, S. R., Hanna, P. C. & Collier, R. J. (1995) *Mol. Microbiol.* **15,** 661–666.
36. Frillingos, S., Sahin-Toth, M., Wu, J. & Kaback, H. R. (1998) *FASEB J.* **12,** 1281–1299.
37. Loeb, D. D., Swanstrom, R., Everitt, L., Manchester, M., Stamper, S. E. & Hutchison, C. A., III (1989) *Nature* **340,** 397–400.
38. Wen, J., Chen, X. & Bowie, J. U. (1996) *Nat. Struct. Biol.* **3,** 141–148.
39. Milla, M. E., Brown, B. M. & Sauer, R. T. (1994) *Nat. Struct. Biol.* **1,** 518–523.
40. Tamura, N., Konishi, S., Iwaki, S., Kimura-Someya, T., Nada, S. & Yamaguchi, A. (2001) *J. Biol. Chem.* **276,** 20330–20339.
41. Sellman, B. R., Nassi, S. & Collier, R. J. (2001) *J. Biol. Chem.* **276,** 8371–8376.